# Systematic variability in ICG recordings results in ICG complex subtypes – steps towards the enhancement of ICG characterization

Sara Benouar [1,2,5], Abdelakram Hafid [1,2], Mokhtar Attari [1], Malika Kedir-Talha [1] and Fernando Seoane [2,3,4]

1. *Laboratory of Instrumentation, University of Sciences and Technology Houari Boumediene, Algiers, Algeria*
2. *Department of Textile Technology, University of Borås, 50190, Borås, Sweden*
3. *Dept. for Clinical Science, Intervention and Technology, Karolinska Institute, 14186 Stockholm, Sweden*
4. *Dept. Biomedical Engineering, Karolinska University Hospital, 14186 Stockholm, Sweden*
5. *Email any correspondence to: sara_benouar-hafid@outlook.com*

## Abstract

The quality of an impedance cardiography (ICG) signal critically impacts the calculation of hemodynamic parameters. These calculations depend solely on the identification of ICG characteristic points on the ABEXYOZ complex. Unfortunately, contrary to the relatively constant morphology of the PQRST complex in electrocardiography, the waveform morphology of ICG data is far from stationary, which causes difficulties in the accuracy of the automated detection of characteristic ICG points. This study evaluated ICG recordings obtained from 10 volunteers. The results indicate that there are several different waveforms for the ABEXYOZ complex; there are up to five clearly distinct waveforms for the ABEXYOZ complex in addition to those that are typically reported. The differences between waveform types increased the difficulty of detecting ICG points. To accurately detect all ICG points, the ABEXYOZ complex should be analyzed according to the corresponding waveform type.

Keywords: bioimpedance, impedance cardiography, dZ/dt signal, ABEXYOZ complex, characteristic points, waveform analysis.

## Acronyms and abbreviations

**ICG**: impedance cardiography
**ΔZ**: impedance change signal
**dZ/dt**: the first derivative of the impedance change signal
**dZ/dtmax**: the maximum amplitude of the dZ/dt signal, also noted as E or C points
**LVET (or ET)**: left ventricular ejection time
**IVRT**: isovolumic relaxation time
**SV**: stroke volume
**CO**: cardiac output

**ABEXYOZ complex:** characteristic points on the dZ/dt signal that constitute one heart cycle
**ECG:** electrocardiography
**PEP:** pre-ejection period
**FT**: ventricular filling time
**STR**: systolic time ratio
**PQRST**: complex in the ECG signal, from P over Q, R and S to T
**ABEX**: segment of an ABEXYOZ complex from A over B and E to X
**YOZ**: segment of an ABEXYOZ complex from Y over O to Z
**FEM:** Finite Element Method

## Introduction

Impedance cardiography (ICG) was introduced in the 1940s [1] as a noninvasive method to measure the mechanical function of the heart. Later, a commercial version of the impedance cardiogram was developed with the support of the National Aeronautics and Space Administration (NASA) [2]. A derivative of the ICG signal, dZ/dt, as shown in Fig. 1, was used to accurately detect ejection time [3] [4]. They demonstrated that the maximum point of the first derivative, dZ/dtmax (noted as point C or E), is related to the rate of ventricular blood ejection [5]. Additionally, to avoid interference in the baseline, the crossing point with the baseline of the dZ/dt signal (noted as the B point) [4] (opening of the aortic valve) was changed to a 15% response of the dZ/dt waveform from the baseline [5].

Another group used the characteristic points of the dZ/dt signal as a simultaneous reference signal for phonocardiogram events [6], suggesting that dZ/dt can also provide a direct characterization of systolic and diastolic time intervals.
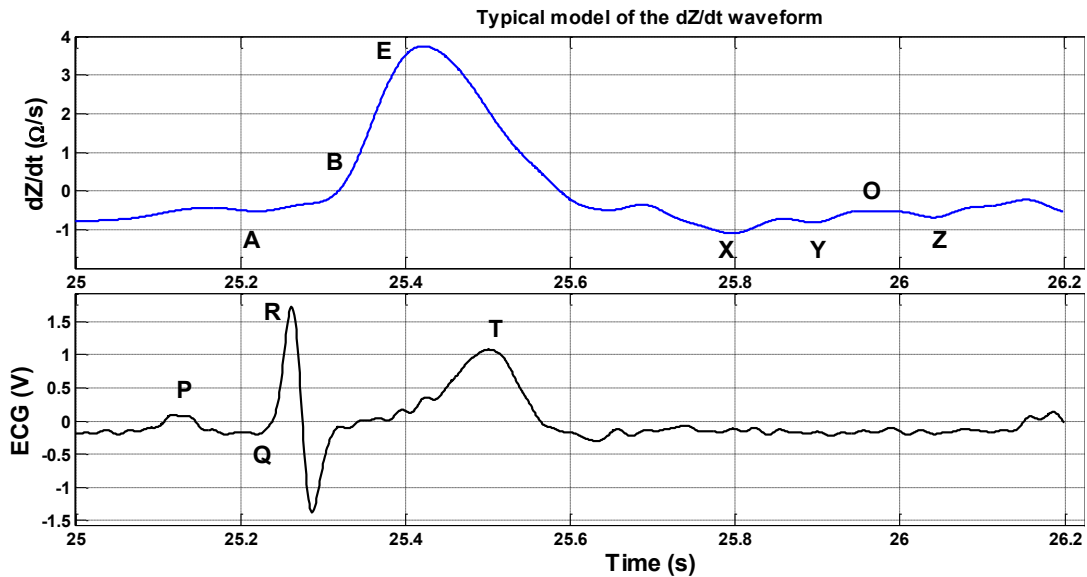
Fig. 1: Typical model of dZ/dt waveform recorded simultaneously with an ECG signal. Each signal is marked by characteristic points.

Therefore, the detection of the characteristic points of the ICG complex of dZ/dt is crucial to calculate several hemodynamic parameters, *e.g., left ventricular ejection time (LVET), isovolumic relaxation time (IVRT), stroke volume (SV) and cardiac output (CO)* [7]. LVET is the time between B and X points in the dZ/dt waveform, which is a crucial element when calculating stroke volume and cardiac output [8]. IVRT is the time between X and O points, which measures the diastolic function and activity of ventricular relaxation [9].

However, in experiments, a straightforward and reliable detection of these time intervals is often problematic [7, 10-12]. The B and X points remain difficult to detect, especially in automated processing, and the principal cause is due to two primary factors: (1) physiological events of the heart are not instantaneous processes, and the time between the opening and closure of aortic valves varies between individuals [13, 14]; and (2) the morphology of the dZ/dt waveform varies considerably in clinical testing. Moreover, there are similar relevant problems for other characteristic points of dZ/dt waveforms [7].

In general, the change in the morphology of the dZ/dt waveform is problematic and leads to unclear conclusions. In a previous study [15], researchers interpreted the wider E wave as an indicator of cardiovascular pathology, with an unclear source of this change. In another study [16], a wider E wave was observed in women with and without a positive index for arterial stiffness. In another study [17], they described the difficulties of automatic analyses due to the motion sensitivity of the ICG waveform and the influence of electrode placement.

From the beginning, authors have raised concerns about certain ICG waveform variability in the recordings [18], suggesting that the observed differences in the morphology of dZ waveforms were primarily caused by the difference in the placement of the electrodes. Recently, other researchers have further studied this phenomenon with 4D

FEM simulations [19, 20] and echocardiographic investigations [21] targeting the influence of lung perfusion, erythrocyte orientation and cardiac pumping on ICG waveforms in addition to aortic volume expansion.

The observed variability between waveform impacts in the accurate detection of specific ICG points, such as point X, has led to the proposal of different detection mechanisms [22] based on different definitions. Moreover, to reduce motion artifacts or changes in ICG waveforms, the ensemble averaging method has been used in impedance cardiograph analyses [23, 24]. This method is performed over time, greater than 60 s, by summing the samples trigged by the R peak and dividing by the numbers of heartbeats in that period [17]. This averaging of heartbeat cycles may result in discarding information that is potentially relevant for ICG analysis.

This study evaluated the changing morphology of dZ/dt waveforms from ICG recordings obtained from two different groups of five healthy, young volunteers. ICG recordings were analyzed to categorize the ABEXYOZ complexes into different waveform cases according to specifically different morphologies. The waveform morphologies of ABEXYOZ complexes may provide a novel perspective of the ICG signal and enable novel alternatives to improve the detection of characteristic points and eventually help to increase the accuracy for estimating hemodynamic parameters.

*ICG recordings and characteristic points of the dZ/dt signal*
The first derivative of the ICG signal impedance change (ΔZ), dZ/dt, is typically represented [6], as shown in Fig. 1, with the 7 characteristic points introduced in Table 1. These characteristic points are critical in calculating certain hemodynamic parameters. Some of these parameters are presented in Table 2 [9], including the requirements for its estimation.

Table 1. Characteristic points of the dZ/dt signal.

| The points | Description |
|---|---|
| A | Atrial contraction |
| B | Aortic valve opening, which is often calculated as a 15% response from the baseline [14]. The B point may also be calculated from an equation that relates the R peak of the electrocardiography (ECG) signal and the E peak of the dZ/dt signal; RB = 1.233RE -0.0032RE2 - 31.59 [11]. |
| E (or C) | Maximum amplitude of dZ/dt from the baseline (dZ/dtmax). It represents the maximum aortic flow. |
| X | Aortic valve closing, which is calculated as the first turning point valley after the E point (d1) or the lowest minimum after the E point (d2) [22]. In the time domain, aortic valve closing occurs at the end of the T wave of the ECG signal. |
| Y | Pulmonic valve closing. It is the minimum notched between the X and O points [6]. |
| O | Mitral valve opening, the maximum positive point after the E wave [6]. |
| Z | Mitral regurgitation, which is the minimum notch after the O point [6]. |

Table 2. Hemodynamic parameters calculated using ICG characteristic points.

| Parameters | Description | Calculation |
|---|---|---|
| PEP | Pre-ejection period | The Q-B segment is required. |
| ET (or LVET) | Ventricular ejection time | The X-B segment is required. |
| IVRT | Isovolumic relaxation time | The X-O segment is required. |
| FT | Ventricular filling time | The Y-Z segment is required. |
| SV | Stroke volume; the volume of blood ejected from the left ventricular in one cycle | Both the E point and X-B are required [8]. $$SV = V_C \sqrt{\frac{E}{Z_0}}\ ET \qquad (1)$$ |
| CO | Amount of blood pumped during 1 min [8] | $$CO = SV \times HR \qquad (2)$$ |
| Heather index | Cardiac contractility index is the ratio between the maximum amplitude of the dZ/dt signal. | Noted E point and the Q-E time interval. $$\text{Heather Index} = \frac{E}{(Q-E)} \qquad (3)$$ |

## Materials and methods

### a) ICG recordings

In this work, two different sets of impedance cardiographs were used. Both sets were recorded at the Laboratory for Medical Textile-Electronics at the University of Borås, Sweden, at two different times with two different recording devices of continuous thoracic bioimpedance and on two different group of volunteers. In both cases, the recordings were performed after participants signed an informed consent form according to the ethical approval, 274-11, granted by the Regional Committee for Ethical Vetting of Gothenburg.

### b) Respimon data

One set of ICG data was obtained in 2013 as described in [25, 26] with a Respimon impedance recorder (Medical Electronics Lab, Chalmers University of Technology, Sweden).

### c) Z-RPI device

A second set of data was acquired with the Z-RPI ICG recorder [27]. It is a custom-made measurement device that simultaneously records a 3-lead ECG and ICG, combining the following system-on-chip (SoC) solutions: the ADAS1000 and the AD5933 from Analog Devices with a Raspberry PI3 card. The Z-RPI ICG recorder is fully described elsewhere [27].

### d) Measurement protocol

To ensure equivalence between ICG measurements performed with both devices, the measurement protocol for the Z-RPI device was adjusted to the measurement protocol executed in previous studies [25, 28]. Measurements were performed in 5 young, healthy volunteers in a seated position while resting using Ag/AgCl gel electrodes. There were a total of N=10 volunteers.

The only difference between the measurement protocols was that ICG recordings with the Z-RPI device were 5 min rather than 60 s. To avoid respiration artifacts, breathing was kept shallow at 10 cycles/min during the recording. Despite the availability of 500 s for each volunteer, the analyses of recordings were limited to 60 s windows.

Both datasets were obtained with Ag/AgCl gel electrodes placed according to a neck-to-chest electrode configuration, as proposed in a previous study [4]. A small shift of electrode placement was introduced (see Fig. 2) to determine whether electrode placement significantly influenced the variability of recordings.

### e) ECG and ICG signal preprocessing

After all ICG and ECG measurements were stored, the recordings were preprocessed offline using MATLAB™, as shown in Fig. 3. Both detrending and filtering functions were applied to both ICG and ECG signals.
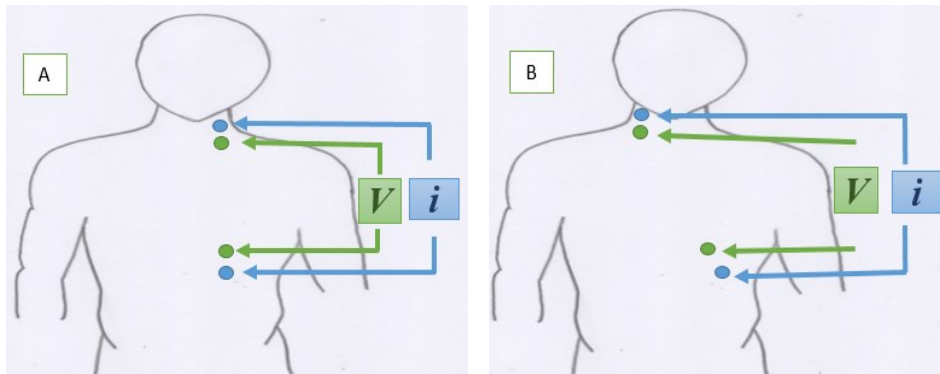
Fig. 2: Electrode positions. a) Electrode positions for measurements obtained with Respimon.
b) Electrode positions for measurements obtained with the Z-RPI device.

Heart rate was obtained from the ECG signal by detecting R-waves and applying the Pan-Tompkins algorithm [28]. The first derivative of the ICG signal was obtained from ΔZ through derivation after smoothing with a low-pass filter with cut-off frequency of 18 Hz (see Fig. 3).

### f) Analysis and visualization

Analyses of the ICG data were performed using MATLAB™ software by first displaying the processed recorded signals and then evaluating the PQRST and ABEXYOZ complexes. ABEXYOZ complexes were detected by the R peaks of the ECG. Then, ABEXYOZ complexes were categorized according to the ICG points.

There were 5 ABEXYOZ complexes that were clearly defined. This categorization enabled the calculation of the percentage of different ABEXYOZ complexes in each group and their distribution among the volunteers. The percentage of each characteristic ICG point in each volunteer was also calculated.

### g) Ethical approval

All procedures performed in this study involving human participants were in accordance with the ethical approval, 274-11, granted by the Regional Committee for Ethical Vetting of Gothenburg.

### h) Informed consent

Informed consent was obtained from all individual participants included in the study.

### Results

Careful analysis of the dZ/dt signal from the acquired ICG recordings presents waveforms with differences in the ABEXYOZ complex when compared to the well-known and well-spread single ICG complex shown in Fig. 1. These differences between complexes were systematic and allow us to classify the waveforms in six different classes, and each of the classes are plotted in Fig. 4a-f, highlighting the observed differences in the presence or absence of the typical characteristic points.

The observed differences can be divided into two types according to which segment of the ICG complex and where they occur (ABEX and YOZ). The ABEX complex includes two potential characteristic points (X1 and X2), where X2 can present two different cases; one of them has not been previously reported.

In Fig. 4, we observed that ABEXYOZ waveforms contain common missing points, where X is missing in the ABEXYOZ types 2, -3, -4 and -5. The Y, O and Z points are missing in the ABEXYOZ types 1, -3 and -4, respectively.
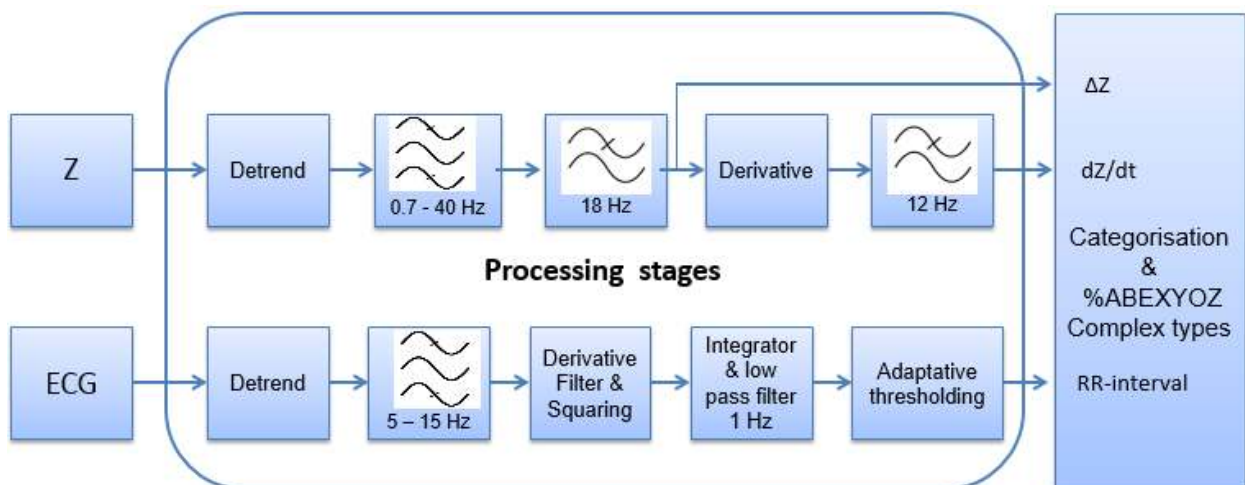


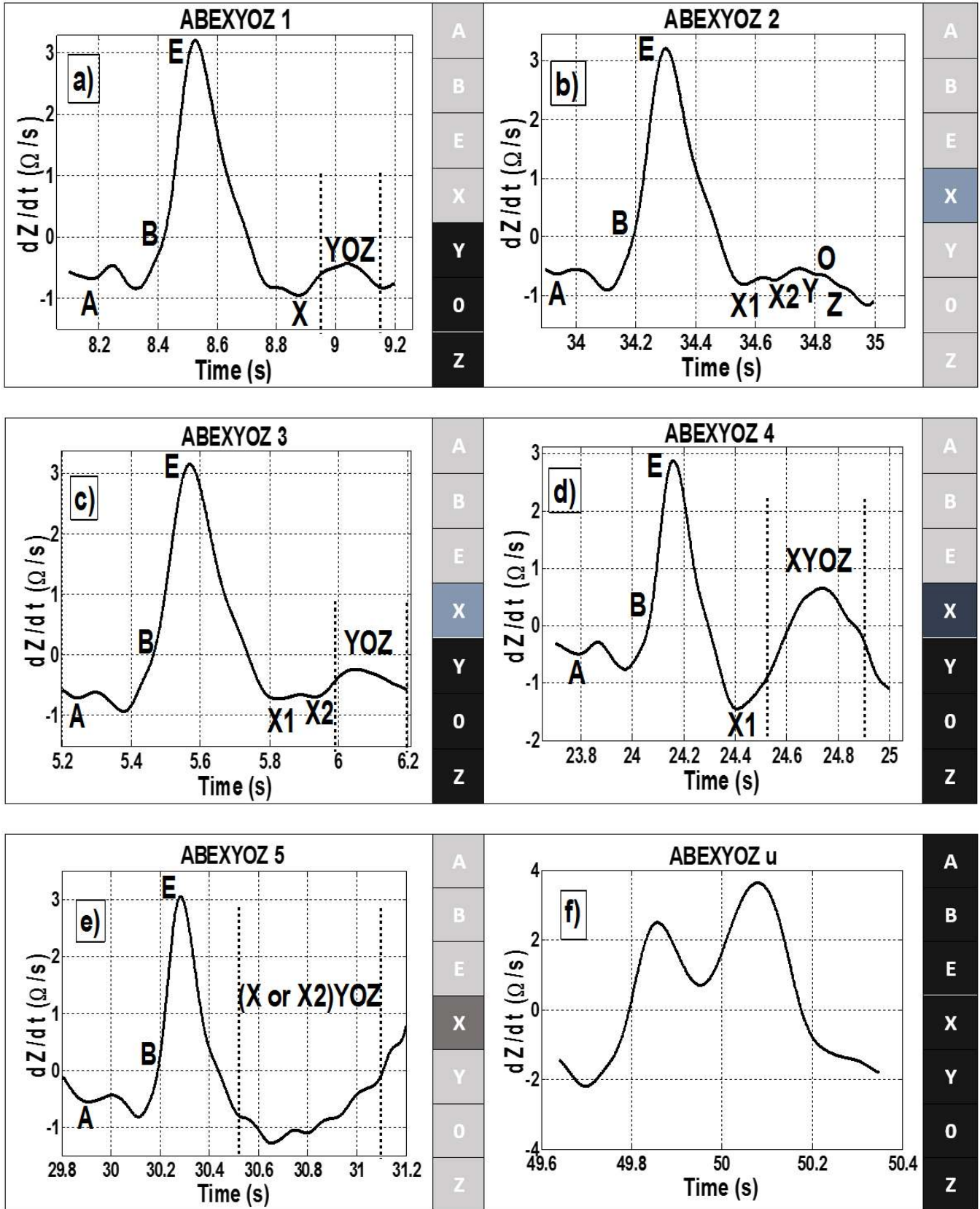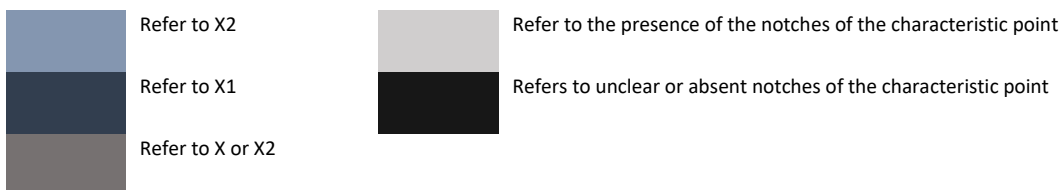Fig. 3: Flowchart of the data processing stages.

Fig. 4: Observed waveform morphology changes (ABEXYOZ types) of the dZ/dt signal.
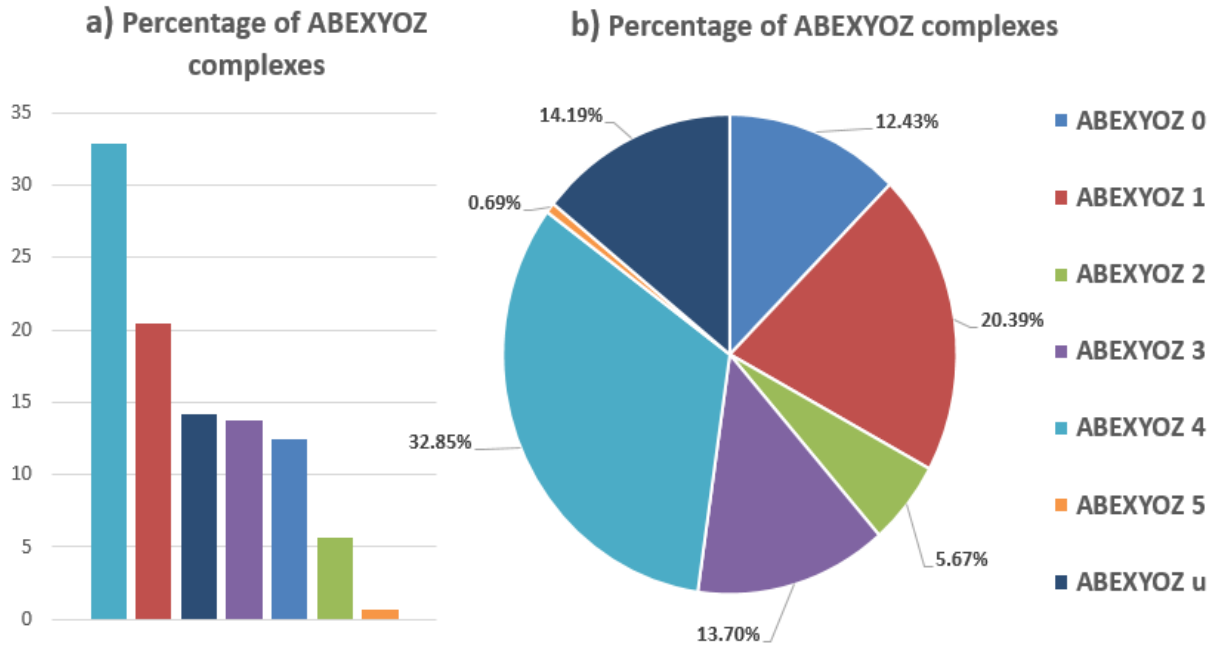
Fig. 5: Distribution of ABEXYOZ complexes with different morphologies.  a) Order of percentages of ABEXYOZ complexes, from the most to the least abundant. b) Percentage of ABEXYOZ complexes.

Fig. 4b and Fig. 4c show ABEXYOZ 2 and ABEXYOZ 3, respectively. The difference between these two complexes is the missing points after X1 and X2. For ABEXYOZ 3, there is one slope for the three YOZ points, which is contrary to the case in ABEXYOZ 2, where the Y, O and Z points can be clearly identified.

The plots in Fig. 4a and Fig. 4d show ABEXYOZ 1 and ABEXYOZ 4, respectively. For ABEXYOZ 1, there is a unique X, but there is one slope that may include all of the YOZ points. For ABEXYOZ 4, there is no X, and there is only one slope that may contain all of the X, Y, O, and Z points.

The plot in Fig. 4e represents ABEXYOZ 5, and we notice a "skirt" waveform, which includes the typical characteristic points, but the morphology of the waveform does not match that of the typical dZ/dt waveform, and the X point is missing on several occasions.

Fig. 4f shows the waveform of an undetermined ABEXYOZ complex (noted ABEXYOZ u). This type of waveform is mainly characterized by a complete absence of most of the ABEXYOZ complexes.

As observed in the plots in Fig. 4, some characteristic ICG points are not present in the ICG waveform. The columns with gray colors on the right of Fig. 4a-f indicate the presence or absence of the typical characteristic points for each of the ABEXYOZ complexes.

The pie chart in Fig. 5 indicates the distribution of the different ABEXYOZ complexes observed in both groups. The distribution was relatively well spread among the different types of waveforms, with ABEXYOZ 4 and ABEXYOZ 1 being the most common waveforms present in the recordings. The waveforms that are the least present are ABEXYOZ 5 and ABEXYOZ 2.

Fig. 6 presents 5-s recordings of a dZ/dt signal, showing five consecutive ABEXYOZ complexes. The morphology

differences between the ABEXYOZ complexes are specifically indicated, with round shapes of discontinuous trace.

Tables 3 and 4 indicate ABEXYOZ waveform types in each volunteer for both groups 1 and 2, respectively. These tables also present the average heart rate (mean ± SD) for each volunteer. Based on the presence of ABEXYOZ types in each volunteer and the absence of characteristic ICG points, Table 5 presents the percentage of absence for each characteristic point observed in the recordings per subject. The absence of characteristic points is reported in three different groups as follows: (1) A, B and E; (2) X; and (3) Y, O and Z. Given the shape of the ICG waveforms as presented in Fig. 4, the frequency of the presence/absence of characteristic points is common between some of the waveforms. For example, A, B and E are always present except in the ABEXYOZ u type waveform. The X point is missing in ABEXYOZ 2, -3, -4 and -5. Y, O and Z are common missing points in ABEXYOZ 1, -3 and -4.

Figure 7 summarizes the total percentage of missing points per group, demonstrating a similar outcome between groups and indicating that the most common characteristic points are present in the first part of the ICG waveform.

## Discussion

### a)  ICG data

In this study, two different sets of ICG recordings were used. They were recorded at two different times with two different groups of volunteers using two different ICG devices. In both groups, the arrangement of electrodes was performed according to the configuration proposed by Kubicek [4], but the actual position of the electrodes was slightly different. The same measurement protocol was

Table 3. Percentage of ABEXYOZ complexes in each recording per volunteer with the average heart-rate (mean ± SD) for group 1

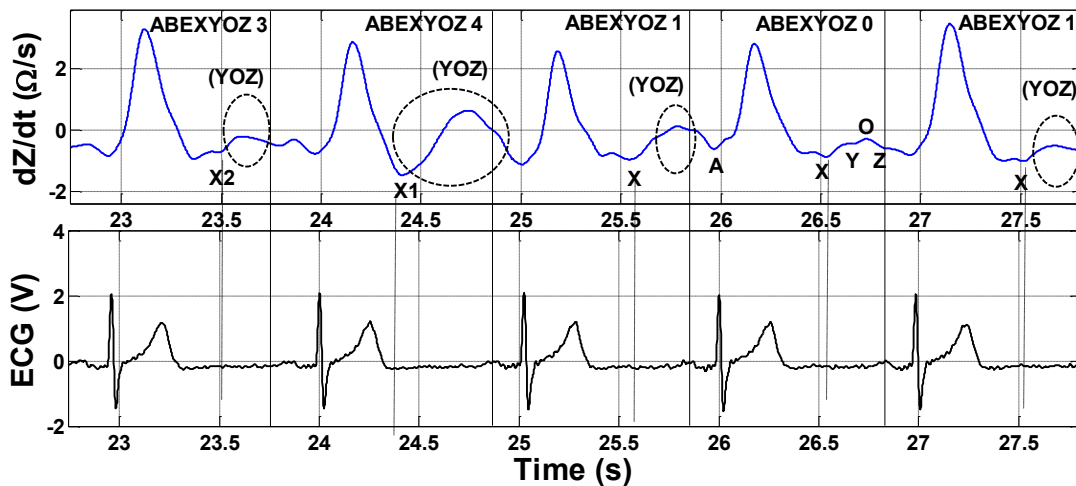| Waveform type for group 1 | 0 | 1 | 2 | 3 | 4 | 5 | u | HR |
|---|---|---|---|---|---|---|---|---|
| V 1 | 72.3 | 04.2 | 02.1 | - | - | - | 21.2 | 55 ± 5 |
| V 2 | 11.3 | 09.4 | 15.0 | 41.5 | 09.4 | 05.6 | 07.5 | 60 ± 3 |
| V 3 | - | 02.7 | - | 08.2 | 53.4 | - | 35.6 | 76 ± 5 |
| V 4 | 01.5 | 01.5 | - | - | 90.6 | - | 06.2 | 66 ± 2 |
| V 5 | - | 03.4 | - | - | 47.1 | - | 49.4 | 90 ± 6 |



Fig. 6: Five consecutive ABEXYOZ complexes with different morphologies.

used for each subject with minor changes, ensuring that valid comparisons could be made while broadening the scope of the study. These non-identical measurement sets enriched the study by incorporating different devices and electrode placements, and despite being not identical, they are equivalent. The measurement sets even presented similar heart-rate ranges despite being collected completely independently and years apart. The different ABEXYOZ complexes were clearly defined by corresponding specific waveforms, which are summarized in Table 6.

### b) ABEXYOZ complex type distribution

The presence of up to five different ABEXYOZ complexes in dZ/dt signals, in addition to the typical and undetermined waveforms, was confirmed. All ABEXYOZ types were present in each of the dZ/dt recordings from both measurement groups. Therefore, we confirmed that (1) all ABEXYOZ complex types are present in dZ/dt recorded signals from the two devices used and (2) all ABEXYOZ complex types are present in the dZ/dt recorded signals from both electrode configurations.

By analyzing Tables 3 and 4, we observed that no specific ABEXYOZ complex seems to be dominant, and the distribution of waveforms differs between groups. However, the distribution of ABEXYOZ complexes varied between different volunteers, with ABEXYOZ 4 dominating among volunteers of group 1 and ABEXYOZ 1 being dominant in those of group 2 (see bar plots in Fig. 7).
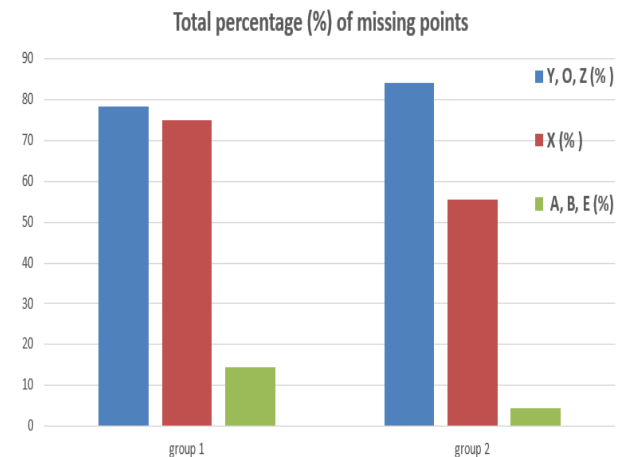


Fig. 7: Total percentage of missing points in both groups.

Given that the volunteers in each group were completely different, these results are expected because specific physiological and cardiodynamic events related to the duration of the opening and closure of the aortic valves vary between people [13]. Variation in the ICG signal between subjects has been previously observed and reported [29]. Therefore, five different ABEXYOZ types were observed in most of the ICG recordings, which were well distributed but not homogeneously distributed. In several ICG recordings, all five different ABEXYOZ types were observed, but in other cases, only two types were observed.

Table 4. Percentage of ABEXYOZ complexes contained in each recording per volunteer with the average heart-rate (mean ± SD) for group 2

| Waveform type Group 2 | 0 | 1 | 2 | 3 | 4 | 5 | u | HR |
|---|---|---|---|---|---|---|---|---|
| **V 1** | - | 86.4 | 02.7 | 02.7 | 08.1 | - | - | 52 ± 4 |
| **V 2** | 29.4 | 06.4 | 23.0 | 10.2 | 15.3 | 01.2 | 14.1 | 75 ± 5 |
| **V 3** | 07.6 | 10.7 | 12.3 | 35.3 | 26.1 | - | 07.6 | 66 ± 7 |
| **V 4** | - | 53.4 | 01.3 | 28.7 | 16.4 | - | - | 69 ± 4 |
| **V 5** | 02.2 | 25.8 | - | 10.1 | 61.8 | - | - | 87 ± 4 |

Table 5. Percentage of missing points of each characteristic point in each volunteer for both groups

| | Group 1 | | | | | Group 2 | | | | |
|---|---|---|---|---|---|---|---|---|---|---|
| | V 1 | V 2 | V 3 | V 4 | V 5 | V 1 | V 2 | V 3 | V 4 | V 5 |
| **A, B, E (%)** | 21.3 | 07.6 | 35.7 | 06.3 | 49.5 | 00.0 | 14.1 | 07.7 | 00.0 | 00.0 |
| **X (%)** | 23.5 | 79.3 | 97.3 | 97 | 96.6 | 13.6 | 64.2 | 81.7 | 46.6 | 72.0 |
| **Y, O, Z (%)** | 25.6 | 68.0 | 100.0 | 98.5 | 100.0 | 97.3 | 46.2 | 80.0 | 98.7 | 97 |

## c) Other specifications of the ABEXYOZ complex types

In the obtained recordings, the less dominant ABEXYOZ complex types were ABEXYOZ 5 and ABEXYOZ 2 in both groups.

Although ABEXYOZ 2 and 5 were not present as often as the rest of the types in the ICG recordings, the observed differences in the YOZ segment clearly indicated that they are both specifically different ABEXYOZ types. They are distinct because a distinguishable X point is missing, which is a remarkable feature given that the X point is critical for calculations of hemodynamic parameters.

The primary difference between the five types of ICG complexes and the typical complex, ABEXYOZ 0, was observed in the second part of the complex after the E wave (the XYOZ segment). Among all of the alterations observed in different ABEXYOZ complexes, the X point varied the most, with the lowest minimum after the E wave. This variability of the X point has led to different definitions of X points, which consequently have produced different detection algorithms, which are tailored to each definition [22]. Additionally, this alteration of the X point has been observed, reported [21] and studied previously [19, 20]. In previous studies [19], [20], the physiological sources that might contribute to building ICG signals (ΔZ and dZ/dt) were investigated.

While it is widely accepted that the main contribution of the ICG signal is produced by aortic expansion, the authors have also shown that the contribution from lung perfusion and erythrocyte orientation cannot be neglected.

Therefore, in the *ABEX complex*, there are three possibilities for point X:

(d1) X, which is a true X point and is defined as typical (see Fig. 1). This point is present as the lowest minimum after the E point. In a previous study [22], it was defined as the lowest minimum in the entire cycle after the E point. This definition can be misleading with the Y point in some cases. However, in some cases, the tailor-made detection

algorithm fixes a percentage from the period of CC intervals to be scanned.

(d2) X1 is the minimum point on the descending slope of the E wave, and

(d3) X is the observed alternative of X2 as an unpronounced X in terms of amplitude (ampX2 < ampX1).

Finally, the *YOZ complex* has missing points that commonly appear or disappear in specific locations.

## d) The X point and ICG patterns

In this study, the typical X point is only present in the typical ABEXYOZ complex, ABEXYOZ 0, and ABEXYOZ 1, as defined in a previous study [6]. In other ABEXYOZ complexes, there are two other wave flexions near the typical X point (X1 and X2). These two flexions are not typical, and they do not refer to a true X point, where true X is considered according the criteria of the lowest minimum flexion after the E wave, as shown previously in Fig. 1 and defined in a previous study [6].

Usually, detecting an X point according to d1 or d2 is misleading; for d1, it may lose the detection of the real X point in terms of time, position and physiological events. For d2, it may detect the Y point and consider it as the actual X point, and in that case, X2 is often present when problems in detecting X arise.

According to physiological events from the ECG, X2 showed the possibility of being an actual X point; therefore, we devised an alternative definition for the X point (d3). In this study, we could account for the number of ABEXYOZ types that includes an X2, which led to approximately 20% of the ICG data representing up to three ABEXYOZ types. More studies in frequency and time analysis should be performed to validate the definition of d3 as a method to detect the X point.

As examples, in the case of ABEXYOZ 4, X1 is the only minimum without any flexion decrease, and in ABEXYOZ 2, -

Table 6. Characteristic pattern of ABEXYOZ waveforms

| ABEXYOZ s | Description of ABEXYOZ complex |
|---|---|
| ABEXYOZ 0 | Typical ABEXYOZ complex of the dZ/dt waveform containing all characteristic ICG points |
| ABEXYOZ 1 | ABEXYOZ complex of the dZ/dt waveform with X but without YOZ are unidentified in one slope |
| ABEXYOZ 2 | ABEXYOZ complex of the dZ/dt waveform with typical characteristic points, except the X point, which is a not a clear X (noted X2) |
| ABEXYOZ 3 | ABEXYOZ complex of the dZ/dt waveform with an unpronounced X point (X2) and no well-defined YOZ points |
| ABEXYOZ 4 | ABEXYOZ complex of the dZ/dt waveform without well-defined XYOZ points that are almost time contained in one slope after the E wave |
| ABEXYOZ 5 | The ABEXYOZ complex of the dZ/dt waveform that have all of the typical characteristic points, except the X point, which may be a true X or X2, and the dZ/dt waveform has a skirt shape. |
| ABEXYOZ u | The ABEXYOZ complex of the dZ/dt waveform that is characterized by a high percentage of noise or missing points |

3 and -5, X2 is not sufficiently pronounced to be the lowest minimum amplitude after the E wave.

In addition to the 5 ABEXYOZ types and the typical ABEXYOZ 0, ABEXYOZ u was present in almost all volunteers. This type of waveform was observed as weakly defined complexes when all typical characteristic points of the dZ/dt signal were missing.

When inspecting the waveforms reported from the simulation work in previous studies [19], [20], among the ABEXYOZ complexes, ABEXYOZ complex 2 improved the reassembling of the waveform and contained contributions from all of the physiological sources, including lung perfusion, erythrocyte orientation and heart rate. Furthermore, the typical ICG complex, labeled here as ABEXYOZ 0, closely agreed with the ICG waveform produced only by the volume changes in the aorta [20].

The ECG recordings were perfectly clear and repetitive, independent of the differences observed in the ICG waveforms. However, all ICG measurements varied between subjects' activities, and repeatable measurements were not possible for all cases [29].

The absence of X has been considered as a pathological instance in a previous study [17] or refers to elderly people. In a previous study [30] with recordings from young healthy subjects, ICG complexes with absent X points were averaged to produce ICG complexes with a clear X point. However, the presence of the X point was achieved at the expense of losing YOZ points.

The observation that the X point is completely absent, i.e., the flexion is not present (X1) or not pronounced as a minimum (X2) in our relatively young and healthy volunteers, suggests that its absence cannot have a pathological source as proposed by other authors [17].

Unlike in a previous study [30], in our study, averaging the ICG produced ICG complexes with clear X points in 6 out of 10 volunteers. Consequently, we did not consider averaging to be a valid alternative to improve the detection of the X point in ICG recordings, especially when the YOZ points were lost in the process as well, as previously reported [30].

### e) ABEXYOZ types and missing ICG characteristic points

The relationship between the ABEXYOZ type and the absence of ICG characteristic points indicates that a difference in the frequency of ABEXYOZ types impacts the absence of ICG characteristic points. Although X is the most common missing ICG characteristic point among the presented ABEXYOZ types, and absent X occurs in 4 out of 5 cases, X is not the most commonly absent point in the obtained ICG recordings. Since both ABEXYOZ 0 (12.43%) and ABEXYOZ 1 (20.39%) contain X points, the absence of a clear X point is limited to 67.18%, while the combined occurrence of ABEXYOZ 1, -3 (13.70%), -4 (32.85), and u (14.19%) ensures the absence of a clear YOZ segment at 81.13%.

The most common set of ICG characteristic points is the ABE segment, and only the ABEXYOZ u case contains no ABE segments. The absence of characteristic points on the ABEXYOZ complexes influences the assessment of hemodynamic parameters from ICG analysis. The estimation of hemodynamic parameters requires the identification of different ICG characteristic points. Left ventricular ET, SV and CO require the detection of both X and B. Other ICG segments or parameters, such as the IVRT and FT, require the accurate detection of X-O and Y-Z, respectively. These last two parameters are important for the diagnosis of diastolic functions of the heart and cardiac malformations.

The currently evaluated recordings suggest that it is possible to directly estimate all hemodynamic parameters of interest (ET, SV, CO, IVRT and FT) in only 12.47% of cases, corresponding to ABEXYOZ 0. Overall, it is possible to estimate the ET, SV and CO in only 32.91% of cases. In only 12.47% and 18.83% of cases, it is possible to estimate IVRT and FT, respectively. Additionally, no parameters can be accurately determined, due to the missing X and YOZ points in ABEXYOZ u, ABEXYOZ 3 and ABEXYOZ 4, in up to 60.74% of cases.

Therefore, to calculate these hemodynamic parameters, it is important to accurately detect ICG characteristic points; therefore, it might be helpful to identify which ABEXYOZ complex types are present in the dZ/dt signal.

## Conclusions and future work

This study reports on waveforms of ABEXYOZ complex types presenting different morphologies to the typical complex expected in ICG recordings. The recorded data clearly exhibited differences for ABEXYOZ complexes in the dZ/dt signal obtained with different devices and from different volunteer groups.

In total, up to five new waveforms for the ABEXYOZ complex of the dZ/dt were identified, and all five complexes were clearly different from the ABEXYOZ complex typically reported in the scientific literature. It was only possible to clearly identify the ICG characteristic points previously defined in the literature in only one of the cases. In the other five cases, at least one ICG characteristic point was missing, and in one case, no characteristic ICG point was detected.

The existence of different ABEXYOZ complexes is important because they impair the use of automatic detection of ICG characteristic points currently based on the assumption and definition of a single ICG pattern. The detection method does not account for waveform specificities associated with the reported variability.

Applying detection methods that are not customized to existing ICG waveforms might lead to estimation errors that will propagate to the calculation of hemodynamic parameters, producing inaccurate values and contributing to the already existing criticism against ICG regarding its limited accuracy and poor robustness [17, 31, 32].

In this study, the types of waveforms present are found in a nonsystematic way, with ICG complexes containing X ICG points intercalated with ICG complexes with missing X ICG points. This type of distribution prompts the use of information from adjacent ICG complexes to improve the detection of X points in ICG complexes without apparent X points.

Therefore, novel ICG waveform algorithms should be developed to improve robustness and accuracy in assessing characteristic ICG points, and we believe that considering the differences among ABEXYOZ complex types presented in this study could improve both robustness and accuracy.

Several approaches that consider the specificities of different ABEXYOZ complex types, combined with descriptive statistics of the time intervals of the ICG segment and its relationships with the PQRST points available from the simultaneous ECG recordings, are currently being tested and will be reported in the future.

## Acknowledgments

## Conflict of interest

Fernando Seoane is a founding director of Z-Health Technologies AB. The rest of the authors declare that they have no conflicts of interest.

## References

1. J. Nyboer, "Bagno, s., Barnett, A, Halsey, RH Radiocardiograms: ElectricalImpedance Changes of the Heart in Relation to Electrocardiograms and Heart Sounds," J. Clin. nves., 19, vol. 963, 1940.

2. W. Kubicek, D. Witsoe, R. Patterson, M. Mosharrata, J. Karnegis, and A. From, "Development and evaluation of an impedance cardiographic system to measure cardiac output and development o5 an oxygen consumption rate computing system utilizing a quadrapole mass spectrometer," National Aeronautics and Space Administration, NASA-CR-92220. (Also N68-32973.), 1967.

3. W. R. Patterson and J. Shewchun, "Alternate approach to the resolution of tunneling current structure by differentiation," Review of Scientific Instruments, vol. 35, pp. 1704-1707, 1964. https://doi.org/10.1063/1.1719283

4. J. Karnegis, W. Kubicek, R. Mattson, R. Patterson, and D. Witsoe, "Development and evaluation of an impedance cardiac output system," 1966.

5. W. Kubicek, R. Patterson, and D. Witsoe, "Impedance cardiography as a noninvasive method of monitoring cardiac function and other parameters of the cardiovascular system," Annals of the New York Academy of Sciences, vol. 170, pp. 724-732, 1970. https://doi.org/10.1111/j.1749-6632.1970.tb17735.x

6. Z. Lababidi, D. Ehmke, R. E. Durnin, P. E. Leaverton, and R. M. Lauer, "The first derivative thoracic impedance cardiogram," Circulation, vol. 41, pp. 651-658, 1970. https://doi.org/10.1161/01.CIR.41.4.651

7. M. T. Allen, J. Fahrenberg, R. M. Kelsey, W. R. Lovallo, and L. J. Doornen, "Methodological guidelines for impedance cardiography," Psychophysiology, vol. 27, pp. 1-23, 1990. https://doi.org/10.1111/j.1469-8986.1990.tb02171.x

8. D. Bernstein and H. J. Lemmens, "Stroke volume equation for impedance cardiography," Medical and Biological Engineering and Computing, vol. 43, pp. 443-450, 2005. https://doi.org/10.1007/BF02344724

9. R. L. Summers, W. C. Shoemaker, W. F. Peacock, D. S. Ander, and T. G. Coleman, "Bench to bedside: electrophysiologic and clinical principles of noninvasive hemodynamic monitoring using impedance cardiography," Academic emergency medicine, vol. 10, pp. 669-680, 2003. https://doi.org/10.1197/aemj.10.6.669

10. A. P. DeMarzo and R. M. Lang, "A new algorithm for improved detection of aortic valve opening by impedance cardiography," in Computers in Cardiology, 1996, 1996, pp. 373-376.

11. D. L. Lozano, G. Norman, D. Knox, B. L. Wood, B. D. Miller, C. F. Emery, et al., "Where to B in dZ/dt," Psychophysiology, vol. 44, pp. 113-119, 2007. https://doi.org/10.1111/j.1469-8986.2006.00468.x

12. J. H. Meijer, S. Boesveldt, E. Elbertse, and H. Berendse, "Method to measure autonomic control of cardiac function using time interval parameters from impedance cardiography," Physiological measurement, vol. 29, p. S383, 2008. https://doi.org/10.1088/0967-3334/29/6/S32

13. M. Handke, C. Jahnke, G. Heinrichs, J. Schlegel, C. Vos, D. Schmitt, et al., "New three-dimensional echocardiographic system using digital radiofrequency data—visualization and quantitative analysis of aortic valve dynamics with high resolution: methods, feasibility, and initial clinical experience," Circulation, vol. 107, pp. 2876-2879, 2003. https://doi.org/10.1161/01.CIR.0000077909.54159.B4

14. W. Kubicek, J. Kottke, M. U. Ramos, R. Patterson, D. Witsoe, J. Labree, et al., "The Minnesota impedance cardiograph-theory and applications," Biomedical engineering, vol. 9, p. 410, 1974.

15. A. P. DeMarzo, "Using impedance cardiography to detect subclinical cardiovascular disease in women with multiple risk factors: a pilot study," Preventive cardiology, vol. 12, pp. 102-108, 2009. https://doi.org/10.1111/j.1751-7141.2008.00012.x

16. T. Kööbi, M. Kähönen, T. Iivainen, and V. Turjanmaa, "Simultaneous non-invasive assessment of arterial stiffness and haemodynamics–a validation study," Clinical physiology and functional imaging, vol. 23, pp. 31-36, 2003. https://doi.org/10.1046/j.1475-097X.2003.00465.x

17. G. Cybulski, "Ambulatory impedance cardiography," in Ambulatory Impedance Cardiography, ed: Springer, 2011, pp. 39-56.

18. K. Sakamoto, K. Muto, H. Kanai, and M. Iizuka, "Problems of impedance cardiography," Medical and Biological Engineering and Computing, vol. 17, pp. 697-709, 1979. https://doi.org/10.1007/BF02441549

19. M. Ulbrich, J. Mühlsteff, S. Leonhardt, and M. Walter, "Influence of physiological sources on the impedance cardiogram analyzed using 4D FEM simulations," Physiological measurement, vol. 35, p. 1451, 2014. https://doi.org/10.1088/0967-3334/35/7/1451

20. M. Ulbrich, J. Muhlsteff, P. Paluchowski, and S. Leonhardt, "Erythrocyte orientation and lung conductivity analysis with a high temporal resolution FEM model for bioimpedance measurements," Lecture Notes on Impedance Spectroscopy: Measurement, Modeling and Applications, vol. 3, p. 71, 2012.

21. P. Carvalho, R. P. Paiva, J. Henriques, M. Antunes, I. Quintal, and J. Muehlsteff, "Robust Characteristic Points for ICG-Definition and Comparative Analysis," in BIOSIGNALS, 2011, pp. 161-168.

22. BIOPAC Systems Inc. (2018). Biopac AcqKnowledge impedance. Available: [Online]: https://www.biopac.com

23. Y. Miyamoto, M. Takahashi, T. Tamura, T. Nakamura, T. Hiura, and M. Mikami, "Continuous determination of cardiac output during exercise by the use of impedance plethysmography," Medical and Biological Engineering and Computing, vol. 19, pp. 638-644, 1981. https://doi.org/10.1007/BF02442779

24. H. Riese, P. F. Groot, M. van den Berg, N. H. Kupper, E. H. Magnee, E. J. Rohaan, et al., "Large-scale ensemble averaging of ambulatory impedance cardiograms," Behavior Research Methods, vol. 35, pp. 467-477, 2003. https://doi.org/10.3758/BF03195525

25. J. C. M. Ruiz, M. Rempfler, F. Seoane, and K. Lindecrantz, "Textrode-enabled transthoracic electrical bioimpedance measurements-towards wearable applications of impedance cardiography," Journal of Electrical Bioimpedance, vol. 4, pp. 45-50, 2013.

26. M. Rempfler, "On the Feasibility of Textrodes for Impedance Cardiography," BIOMEDICAL ENGINEERING, University of Borås, 2011.

27. A. Hafid, S. Benouar, M. Kedir-Talha, F. Abtahi, M. Attari, and F. Seoane, "Full Impedance Cardiography measurement device using Raspberry PI3 and System-on-Chip biomedical Instrumentation Solutions," IEEE Journal of Biomedical and Health Informatics, 2017.

28. J. Pan and W. J. Tompkins, "A real-time QRS detection algorithm," IEEE transactions on biomedical engineering, pp. 230-236, 1985. https://doi.org/10.1109/TBME.1985.325532

29. S. Thomas, "Impedance cardiography using the Sramek-Bernstein method: accuracy and variability at rest and during exercise," British journal of clinical pharmacology, vol. 34, p. 467, 1992.

30. N. C. S. Capela, "IMPEDANCE CARDIOGRAPHY," University of Coimbra, 2013.

31. G. Cotter, A. Schachner, L. Sasson, H. Dekel, and Y. Moshkovitz, "Impedance cardiography revisited," Physiological measurement, vol. 27, p. 817, 2006. https://doi.org/10.1088/0967-3334/27/9/005

32. M. Ulbrich, P. Paluchowski, J. Mühlsteff, and S. Leonhardt, "High temporal resolution finite element simulations of the aorta for thoracic impedance cardiography," in Computing in Cardiology, 2011, 2011, pp. 149-152.